J11.3. REMOTE SENSING OF ATMOSPHERIC AEROSOL PROPERTIES

C. Russell Philbrick[1], Hans Hallen, Michelle Snyder
North Carolina State University, Raleigh NC
Andrea M. Brown
Johns Hopkins University, Applied Physics Laboratory, Laurel, MD

1. INTRODUCTION

Ambient aerosol properties and distributions are still one of least understood features of the lower atmosphere. A new technique has been developed that promises to help fill the voids in this knowledge during the next several years. Based on ideas we considered in the mid-1980s, several doctoral students have developed and applied the capabilities of using the polarization ratio of the optical scattering phase function to determine the properties of atmospheric aerosols. Bistatic and multistatic lidar measurements use the polarization ratio of the scattering phase function to calculate profiles of the aerosol number density, size distribution, and type. These parameters can be determined for spherical particles in the size range between about 20 nm and 20 μm using UV-VIS-NIR wavelengths. Analysis of the aerosol concentration and size distribution requires adopting a mathematical shape function, usually a log-normal distribution of spherical particles. Information on aerosol type can be roughly determined based on the refractive index of the scatterers and depolarization of the scattered radiation as a function of wavelength. Measurements have been used to investigate vertical profiles of layered haze and determine the properties, and horizontal measurements have been used to characterize the aerosols for different types of fog. One project has studied the cases of relatively dense fogs, where multiple scattering dominates. Laser remote sensing techniques provide important tools to determine most of the characteristics of aerosols, including their physical and chemical properties. Spatial and temporal distributions of aerosols are then available to investigate the sources, processes of formation, growth rate, and the roles aerosols play in establishing the planetary albedo and radiative transfer into space.

Laser remote sensing techniques can now provide tools for investigations of most of the properties of aerosols, including their physical and chemical characteristics. Examples from several data sets are selected to show the types of information contained in the optical scattering signatures. These measurements improve our understanding of the distribution of aerosols, their sources, and processes controlling their formation and growth are needed for a detail understanding of their contributions to the planetary albedo and their influence on radiative transfer.

Several laser remote sensing techniques are used to characterize the properties of aerosols. The various techniques include: the Rayleigh lidar profiles of relative backscatter coefficient, profiles of optical extinction using Raman scatter, and bistatic-multistatic scattering using the polarization ratio of the scattering phase function. In addition, the Raman lidar can provide simultaneous profiles of water vapor and temperature so that the growth of hydroscopic aerosols can be examined. Bistatic and multistatic lidar measurements of the polarization ratio are used to determine the number density, size, and size distribution, under the assumption of spherical scatterers. The measurements can sometimes be used to describe other aerosol characteristics; properties such as aerosol type based upon approximate refractive index, and departures from spherical shape particles, can be determined when several wavelengths and multiple angles are available in simultaneous data sets, and when the aerosol environment is not too complex in containing several overlapping size distributions.

2. RAYLEIGH AND RAMAN SCATTERING

Backscatter measurements from Rayleigh and Raman lidar provide signals to profile the properties that govern the transmission of radiation through an atmospheric column. A six-hour sequence of profiles from a micropulse Rayleigh lidar is shown in Fig. 1. Here the aerosol backscatter coefficients show the aerosol scatter during a normal morning rise of the planetary boundary layer. In the troposphere, the direct

* *Corresponding author address:* C. Russell Philbrick, NC State University, Physics Department, Raleigh, NC 27695-8202; e-mail: philbrick@ncsu.edu

backscatter optical signals of laser beams from the mixture of molecules and aerosols provides limited information; such measurements are useful for primarily describing cloud ceiling, relative backscatter coefficient, and for detection of the presence of aerosol and cloud layers.

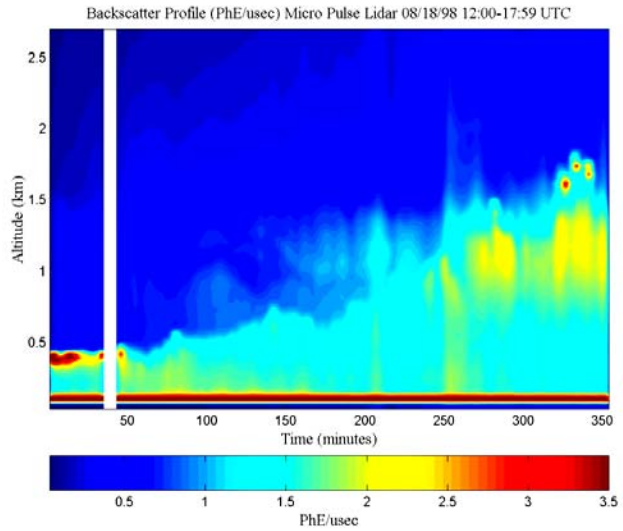

Figure 1. Aerosol scattering between 8AM and 2PM local time from a micropulse Rayleigh lidar (SESI) shows the growth of the boundary layer (Mulik, 2000).

Raman lidar provides important capabilities by measuring concentration profiles of major species, as well as profiles of optical extinction, thermodynamic properties, temperature and dynamics of a tracer. The profiles of all major molecular species (N_2, O_2, H_2O) and several minor species (O_3, CO_2) are measured simultaneously, temperature profiles are measured using rotational Raman scattering, dynamical processes studied using tracers such as water vapor, and aerosol extinction is directly measured using the gradients in the vertical profiles of the molecular constituents (O'Brien et al., 1996; Philbrick, 2002; Li, et al., 2002; Philbrick, 2005).

Raman lidar backscatter from the major molecular components is analyzed to provide extinction profiles. Ratios of simultaneous measurements of extinction and backscatter are used to classify the aerosol types. Analyzing the gradients in the vertical profiles of the vibrational Raman signals of N_2, O_2, and the rotational Raman molecular signals, and comparing them with those expected for the hydrostatic profile of the molecular atmosphere provides robust profiles of the optical extinction at several wavelengths, such as those shown in Fig. 2. The profile of the temperature of the molecular atmosphere is obtained using the measured rotational Raman temperature profile. As expected, the profiles of different wavelengths all approach the same value when multiple scattering properties begin to dominate, as in the layers observed at 4.5 and 5.5 km in Fig. 2. Extinction profiles for several wavelengths are quite are used to observe changes in the particle size, as a function of altitude and time. In the case of shown in Fig. 2, the relative extinction of the different wavelengths (284, 530 and 607 nm), exhibit changes in time and space as the particle sizes increase in the upper aerosol layers, where multiple scattering by large particles occurs.

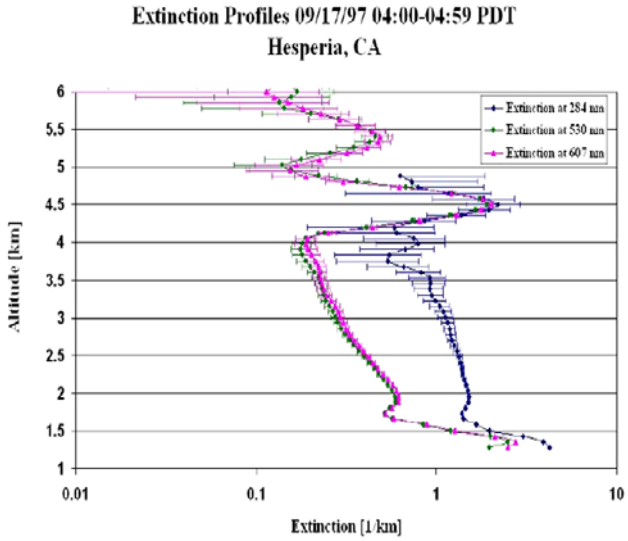

Figure 2. Vertical extinction profiles from gradients in the vibrational Raman profiles of N_2 at 284 and 607 nm, and rotational Raman scattering profiles of the integrated band at 530 nm are shown (Philbrick, 2005, Verghese et al., 2005).

Further comparisons of the ultraviolet and visible wavelength extinction profiles are shown in Fig. 3, as the evolution of cloud occurs as a function of time. The vertical profiles are smoothed using a 5-minute filter to provide set of results shown in Fig. 3. The extinction at both visible and ultraviolet wavelengths are shown on the same scale. The 284 nm ultraviolet measurement clearly exhibits the smaller particles distributed around cloud. Studies using UV and VIS wavelengths make it possible to follow the growth and dissipation of clouds.

Figure 4 shows the time sequence of water vapor and optical extinction profiles during the early development of a cloud, which is sub-visual in these initial stages. The evolution in a developing cloud is first detected as an increase in the water vapor concentration; later the aerosols

are detected as ultraviolet extinction, and still later as extinction at visible wavelengths.

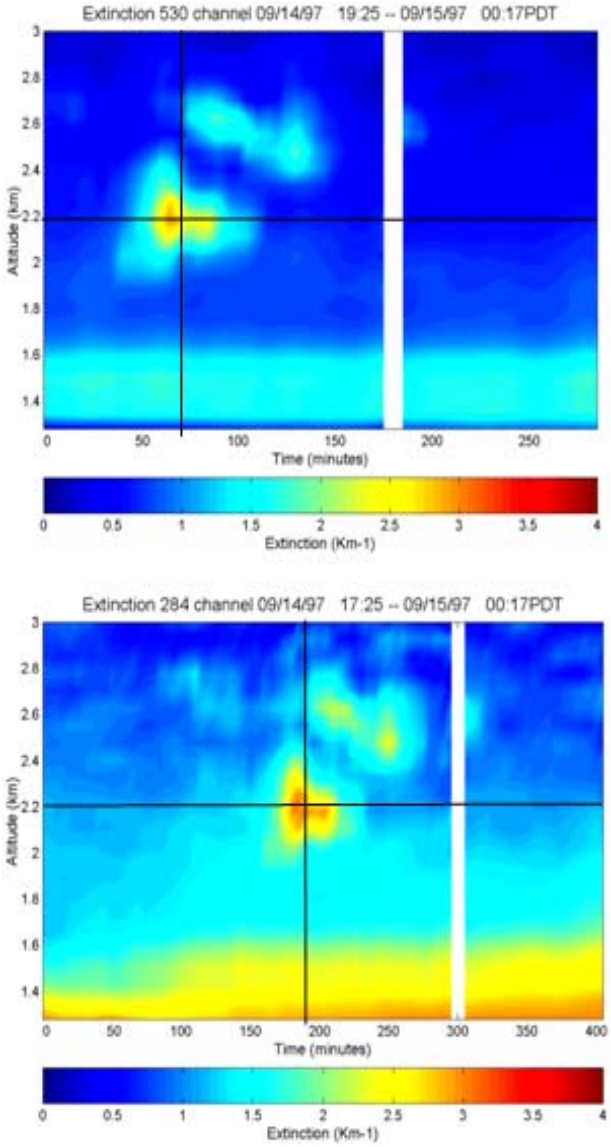

Figure 3. A time sequence of optical extinction profiles shows a cloud moving through the vertical lidar beam; (a) visible (530 nm), (b) ultraviolet (284 nm). The ultraviolet extinction shows the regions of smaller particles surrounding the thin clouds, and the small particle haze layer that was present near the ground, and lines locate a point of simultaneous measurements (Li et al. 2002 and Verghese et al. 2005).

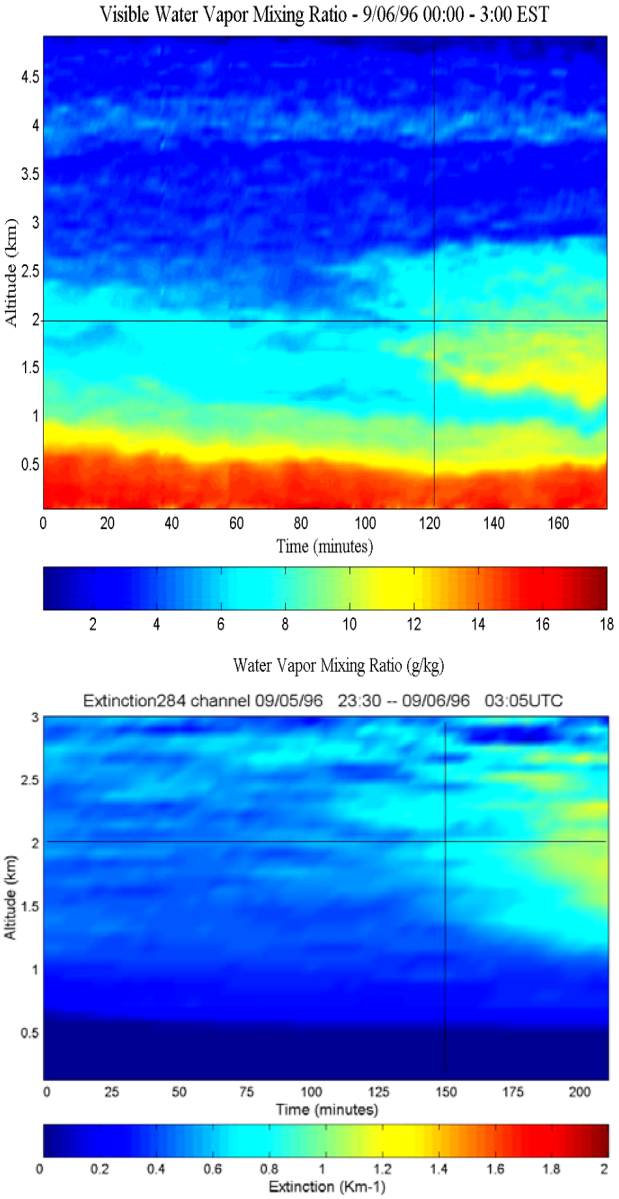

Figure 4. (a) Time sequences of water vapor profiles indicate the development of a cloud occurs before it is evident in the extinction profiles shown in (b); the lines are added to assist in locating corresponding points (Li et al. 2002, Philbrick et al 2005, Verghese et al. 2005).

Figure 5 presents a figure prepared for an investigation of cloud processes. It uses a time sequence of optical extinction from ultraviolet and visible wavelengths, where enhanced scattering by smaller particles is observed in the shorter wavelength (UV) plot. The extinction scales for both plots are the same. The optical extinction values become comparable within the cloud where large particle multiple scattering dominates, refer back to see this effect in Fig. 2.

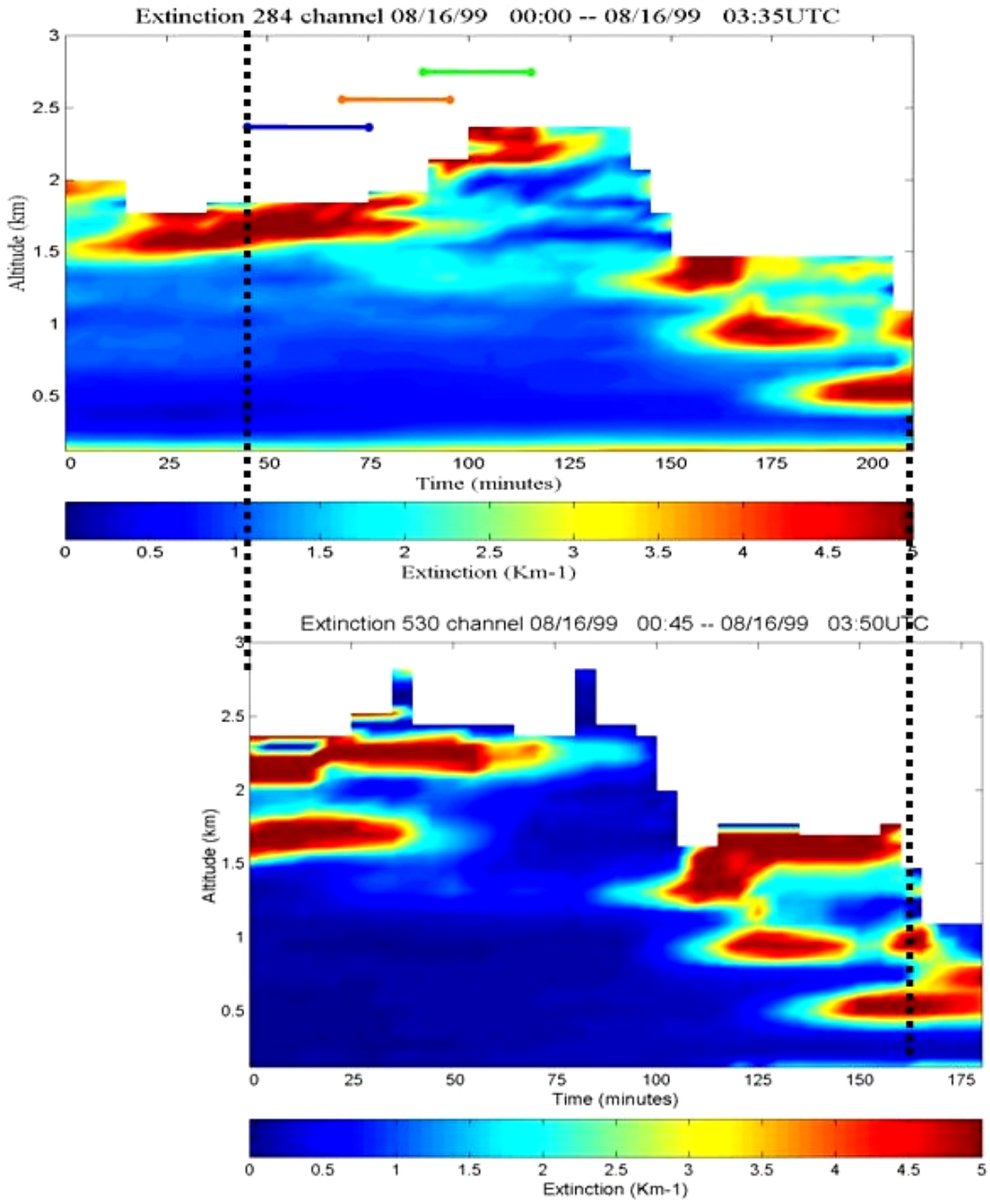

Figure 5. Time sequences of cloud scattering, at ultraviolet (284 nm) and visible (530 nm) wavelengths show the locations of scattering from smaller particles surrounding the clouds (Verghese et al. 2005, Verghese 2008).

The simultaneous Raman lidar measurements of water vapor and temperature obtained during a 6-hour period on the USNS Sumner during tests in the Gulf of Mexico are shown in the left-hand panels of Fig. 6. These two data sets are used to directly calculate the relative humidity, which is shown in the upper right panel. The optical extinction in the lower right panel was determined from the gradients in the N_2 Raman scatter profile generated by the 266 nm Nd:YAG laser. When the measurements of optical extinction are compared with the relative humidity, we see the relationship between the regions where aerosols and clouds form in regions of higher humidity. In Fig. 6, the water vapor plot terminates on the right side when the optical extinction causes the error in the measured value to exceed a set threshold. The extinction plot in the lower right confirms that this is caused by the extinction of the aerosol cloud located there.

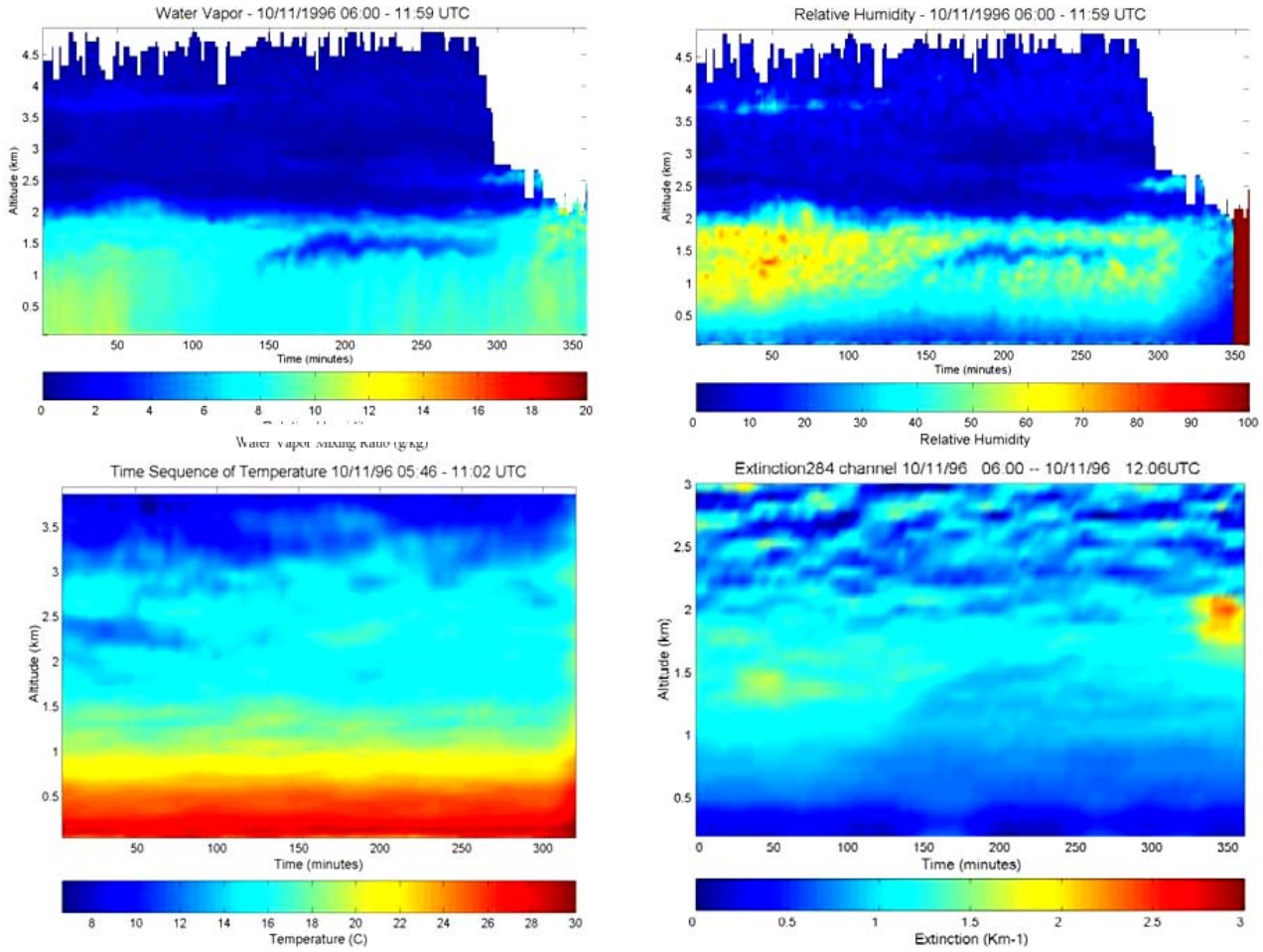

Figure 6. The parameters measured by the Raman lidar, water vapor and temperature (left side) are used to calculate the relative humidity, and this can be compared with the measured extinction to examine the regions of haze and cloud formation (Philbrick 2005).

3. AEROSOL SCATTERING

The previous section shows examples demonstrating that the optical extinction profiles obtained directly from gradients in the molecular profiles of the primary molecular constituents. The gradients measured in the lidar signal are compared with the hydrostatic profile if looking vertical and with the $1/r^2$ dependence if measured horizontally. The same laser beam that is used for vertical or horizontal Raman lidar measurements can also be imaged from a side angle to obtain bistatic lidar data, which is analyzed using the scattering phase function to determine more details regarding the aerosol properties. Figure 7 shows a classic picture of the scattering phase function for two polarization planes, and depicts Mie scattering conditions. These cases show the intensity of the scattered radiation increases and the pattern becomes more complex as the ratio of the particle size to the wavelength increases. A set of pictures of the optical scattering from different directions are shown in Fig 8. The scattering phase function of each polarization (perpendicular or parallel with the plane containing the beam and sensor) can be measured from digital images of the beam. The intensity of the scattering was used to study aerosol properties earlier (Reagan et al. 1982a, 1982b). These investigations make use of the polarization ratio of the scattering phase function to minimize uncertainties from the extinction along paths between the scattering volume and the sensors. Figures 9, 10, and 11 show results from a series of tests designed to demonstrate this capability by using bistatic lidar measurements to describe aerosol properties (Novitsky and Philbrick, 2005; Stevens 1996; Novitsky 2002).

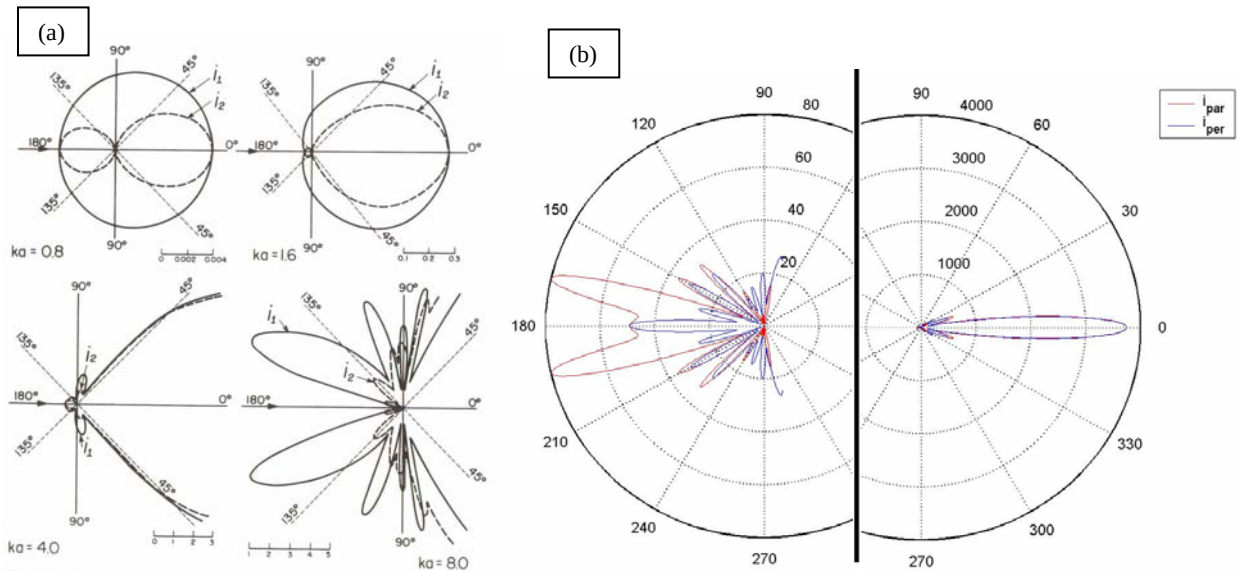

Figure 7. (a) The angular variation of the intensity of the scattering phase function is shown for both polarizations and several cases of ka = $2\pi a/\lambda$ (a is the particle size and λ is the scattering wavelength) (Born and Wolf, 2002); (b) polar plot of the scattering phase function for the two polarization components is shown for the case of 1 μm diameter particles illuminated with 532 nm wavelength laser beam; the LHS shows a magnified scale of the backscatter intensity.

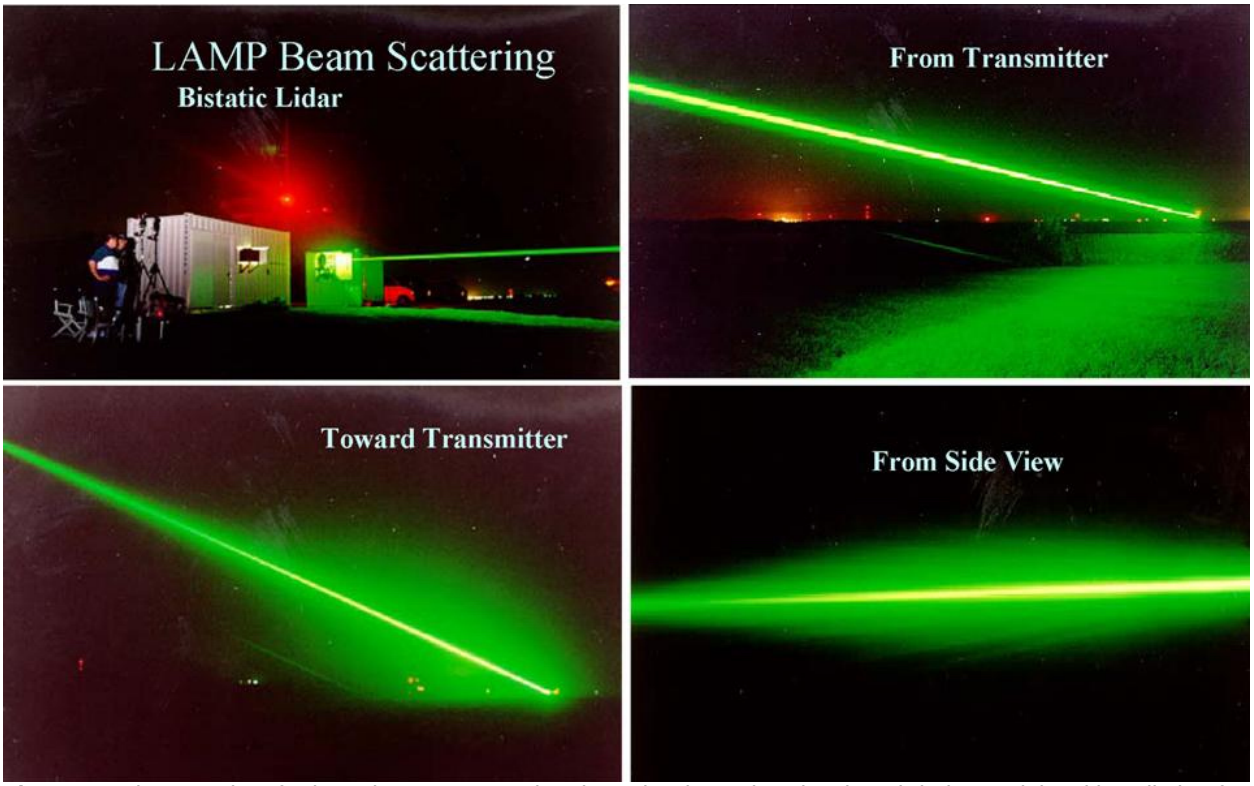

Figure 8. Photographs of a laser beam propagating through a haze that developed during a night with radiation fog (Philbrick). The views of the arrangement include looking along the beam, back toward the transmitter, and from the side show the intensity distributions scattered from the laser beam propagating through a light radiation fog.

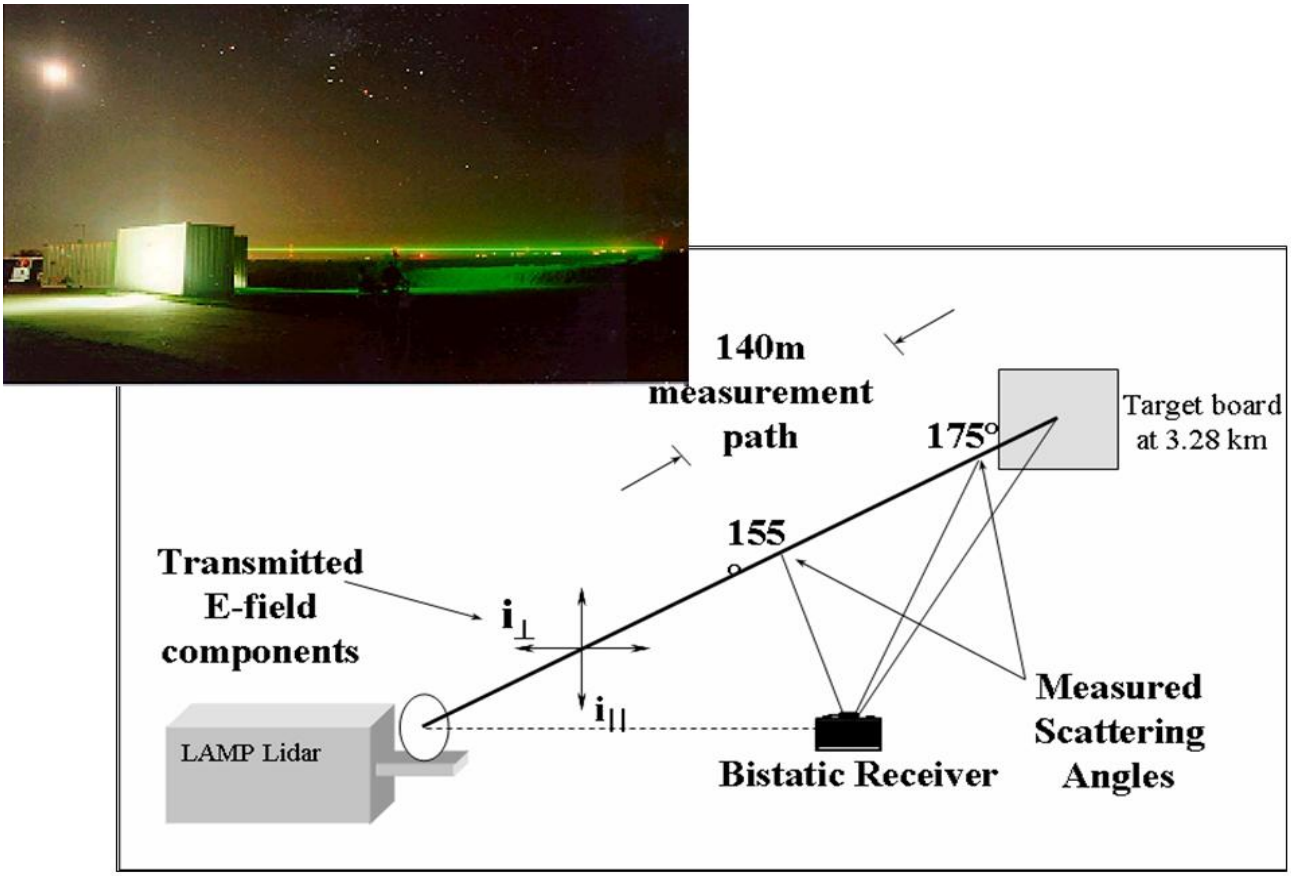

Figure 9. Arrangement used for the bistatic lidar measurements during the CASES project at NASA Wallops in September 1995. The measurements were made using the LAMP Raman lidar which measured optical extinction on the path (Stevens and Philbrick 1996 a, b; Stevens 1996).

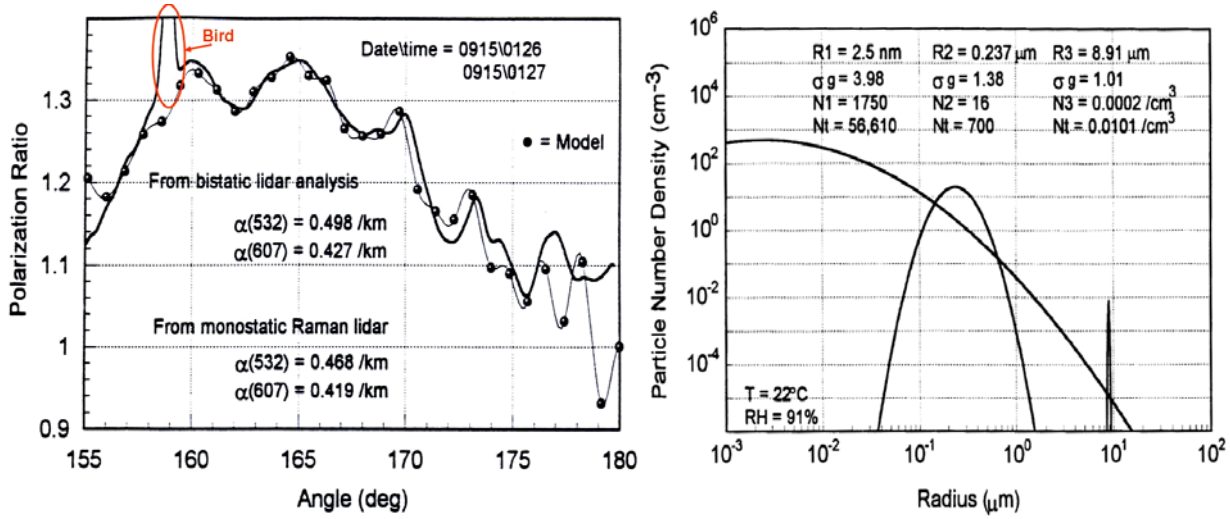

Figure 10. (a) Polarization ratio from the measured intensities is compared with calculations from the best fit solutions of the Mie equations; (b) the solution for the results in (a) are shown for fitting these tri-modal distributions to determine the density and size (peak and distribution width) -- the peak at 9 μm contributes most to scattering (Stevens and Philbrick 1996 a, b; Stevens 1996).

Our early approach for bistatic measurements was to make use of the high power Raman lidar beam. Research campaigns have used horizontal paths with end-points on hard targets, like the one shown in Fig. 9, and vertical measurements using several receivers to resolve layered structures, as shown in Fig 11. Vertical measurements of the Raman lidar provide an ideal configuration for making multi-static measurements of the aerosol profiles. It was found that vertical measurements require simultaneous data at two or more angles to analyze the aerosol properties. The system uses imaging detectors to measure the intensity as a function of angle, and the detectors are placed along radials on the planes of the parallel and perpendicular polarization of the laser transmitter. If one radial is used, the polarization plane can be flipped 90^o by inserting a polarization rotator. Measurements of the two polarization components are normally obtained within a period of a few seconds (optical shutter times are a fraction of a second to a couple of seconds), and data sets are typically obtained in a sequence at a rate of about once per one to five minutes.

An example from the bistatic measurements and analysis results from the CASES experiment is shown in Fig. 10. In Fig. 10(a), the polarization ratio formed from the intensities of each pixel interval in the imaging array is plotted versus angle. The data for angles near 180^o does not contain significant information on the phase function. The analysis uses an array calculated from the Mie equations of aerosol scattering for spherical particles and finds the best match for a tri-modal distribution of particles. The free parameters to be fit are the mean size and distribution of sizes, and the number densities for the three modes. The polarization ratio from the best fit solution for this particular case are plotted as points along with the measurements in Fig. 9(a). In addition to the assumption of spherical particles, an assumption for the size distribution is necessary; we have selected the log-normal distribution. Another parameter that can be estimated from the analysis is the index of refraction. Figure 10(b) shows the solution for data in Fig. 10(a). The best fit parameters for this case are shown in the top of Fig. 10(b). The integrated extinction that would be caused by the scattering particles can be calculated for any wavelength using the results for the density, size, size distribution and index of refraction of the particles. The optical extinction values at 532 and 607 nm corresponding to the solution in Fig. 10(b) are compared with the independent measurement by the Raman lidar in the inset of Fig. 10(a). The values obtained from the Raman lidar measurements obtained at the same time for the extinction values differ by about 5%, and are within the measurement error (Stevens 1996; Stevens and Philbrick 1996).

4. MULTISTATIC SENSING OF AEROSOLS

The developments of the analysis of vertical profiles required a different approach to resolve the profiles of the vertical structure through the often present aerosol layers. The key to obtaining accurate results is to further constrain the solution by making measurements at several different angles simultaneously in the overlapping field-of-view (fov) from several imagers; four or five locations along the radial are preferred. The angles can be determined accurately in the case when the end-point of the vertical beam is contained in the fov; also the star field can be imaged at night. The angles for horizontal measurements can also be obtained by suspending a string above the beam with small wires suspended to reflect points in the beam when jiggled. The imagers are fitted with band filters for the laser wavelength (532 nm was used in this case), but the bandwidth cannot be too narrow or it limits the angular acceptance. Future configurations will make use of confocal optics to allow use of narrow band filters and permit measurements in higher background conditions. Figure 11 shows the arrangement that was used to acquire the vertical multistatic lidar measurements (Novitsky 2002; Novitsky and Philbrick 2005). Experience has indicated that three to five overlapping images are needed to provide sufficient resolution in regions where large gradients in the aerosol density exist on the edges of aerosol layers. The simultaneous measurements of several angles at each pixel height remove the ambiguity in the solution. Figure 13 shows a data set that was obtained for a low altitude layer of aerosols and fit with a bi-modal size distribution.

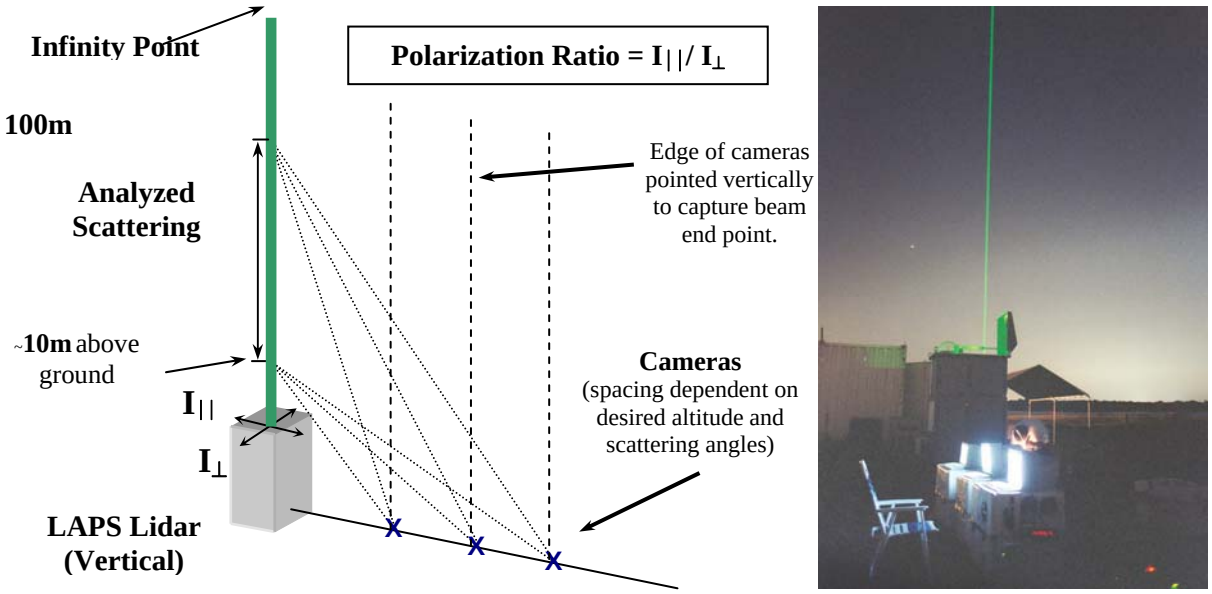

Figure 11. Arrangement for the multistatic lidar measurements is shown (Philbrick 2002; Novitsky and Philbrick 2005).

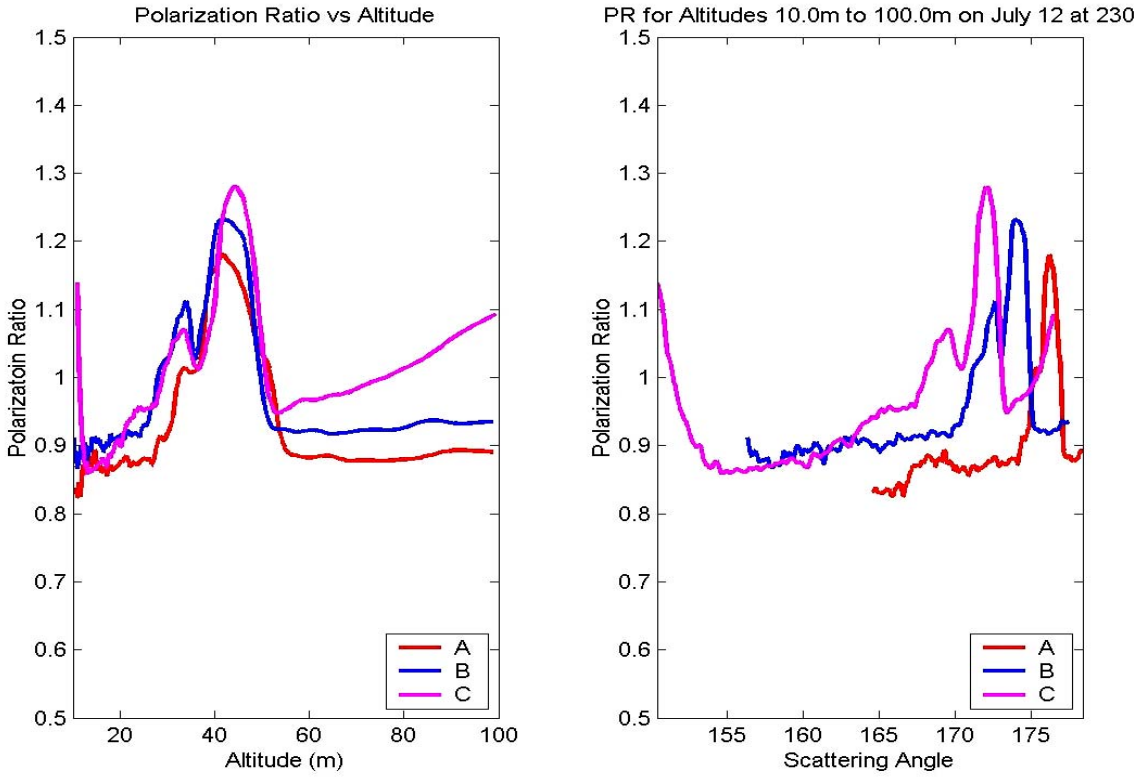

Figure 12. A low altitude aerosol layer is investigated with the multistatic lidar. The figures show the polarization ratio plotted versus altitude and scattering angle (Novitsky 2002; Novitsky and Philbrick, 2005).

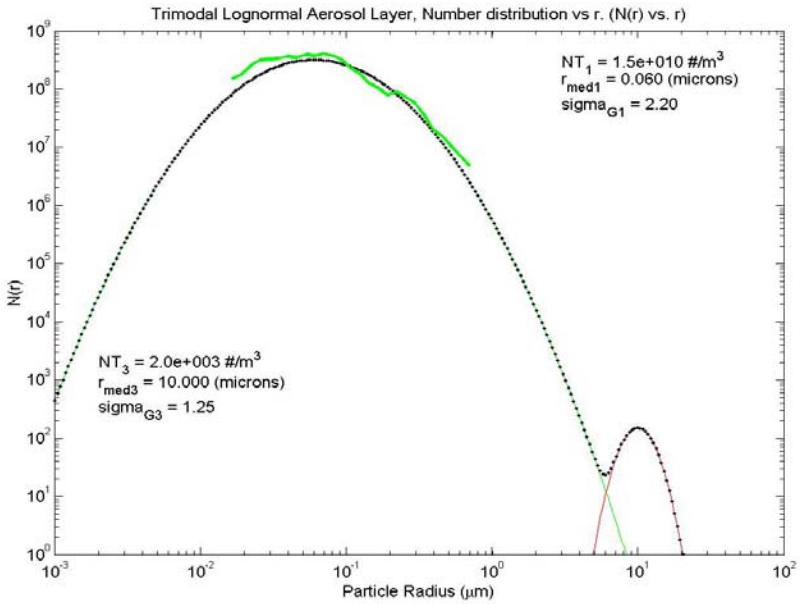

Figure 13. Analysis of this multistatic lidar data was best fit with a bi-modal size distribution with 60 nm and 10 μm particle size distributions (Novitsky 2002; Novitsky and Philbrick, 2005).

5. MULTI-λ MULTISTATIC LIDAR

Recent experiments have added multiple wavelengths to the multistatic arrangement to improve the fidelity of the result and to extend the applicable size range of the particles that can be measured. The useful range for the scattering polarization ratio of phase function analysis is found to be for particles approximately of range of sizes, $0.1 < \lambda < 10$. The several wavelengths are measured simultaneously by co-aligning the beams of three lasers and using a diffraction grating in front of the imager to record the separated wavelengths in first order. Laboratory experiments using chambers have been used to test the analysis approach and evaluate various aspects of the measurement. The advantage of using the polarization ratio of the phase function is that most of the unknowns in the lidar equation cancel as in the polarization ratio equation,

$$\delta_p = \frac{P_{r,\parallel}}{P_{r,\perp}} = \frac{P_t \frac{C}{D} \beta_\parallel(z,\theta) T^2 d\theta}{P_t \frac{C}{D} \beta_\perp(z,\theta) T^2 d\theta} = \frac{\beta_\parallel(z,\theta)}{\beta_\perp(z,\theta)}$$

Figure 14 shows an example of the angle variations in the scattering phase function and the polarization ratio when water aerosols with a mean diameter of 1 micron and a geometric standard deviation of 1.2 scatter a 650 nm laser beam. A wider distribution of particle sizes reduces the definition of the structure features in the result and can reduce the accuracy of the result. By using multiple wavelengths and multiple view angles, we expect to be able to evaluate the quality of the answer since each wavelength can be considered as a mostly independent solution.

An experiment was conducted in the EPA Aerosol chamber in Research Triangle Park NC during November 2009. The experiment used oil aerosols that were characterized by an APS as having a mean diameter less than 500 nm. The polarization ratio measured and calculated for the scatter of three laser wavelengths of 405, 532 and 650 nm measured in the PSU chamber is shown in Fig. 15. Figure 16 shows the results obtained for the three wavelengths measured during two of the experiments at the EPA Chamber, together with calculations of the expected polarization ratio for the total particle concentrations and size distribution inverted from the measurements. Figure 17 shows the structure in the polarization ratio for 1 μm diameter polystyrene spheres recorded simultaneously using two imagers with diffraction gratings viewing at two overlapping angle ranges in an aerosol chamber constructed at the NCSU Lidar Laboratory.

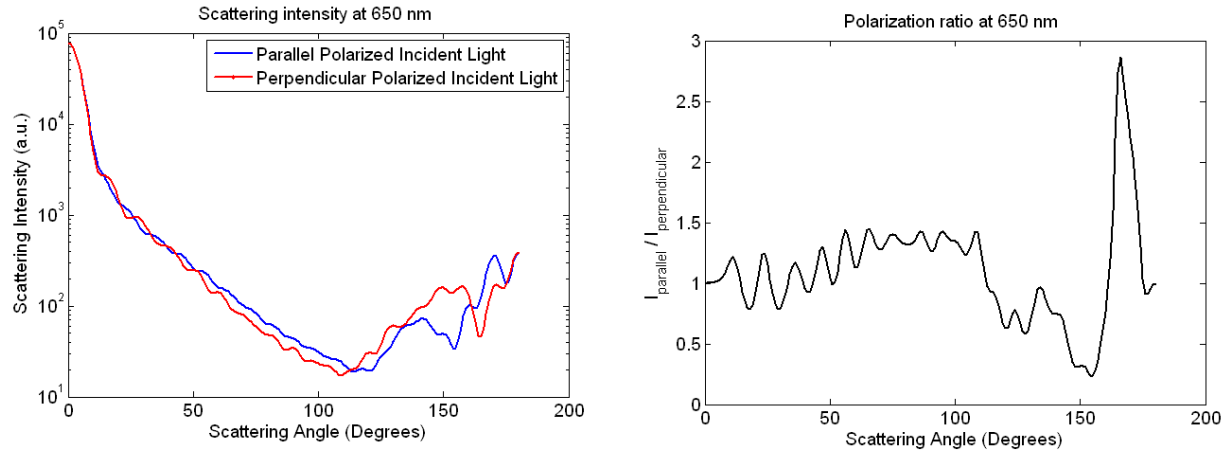

Figure 14. Plots show the calculated variation in the scattering phase function and the polarization ratio when water aerosols with a mean diameter of 1 micron and a geometric standard deviation of 1.2 scatter a 650 nm laser beam.

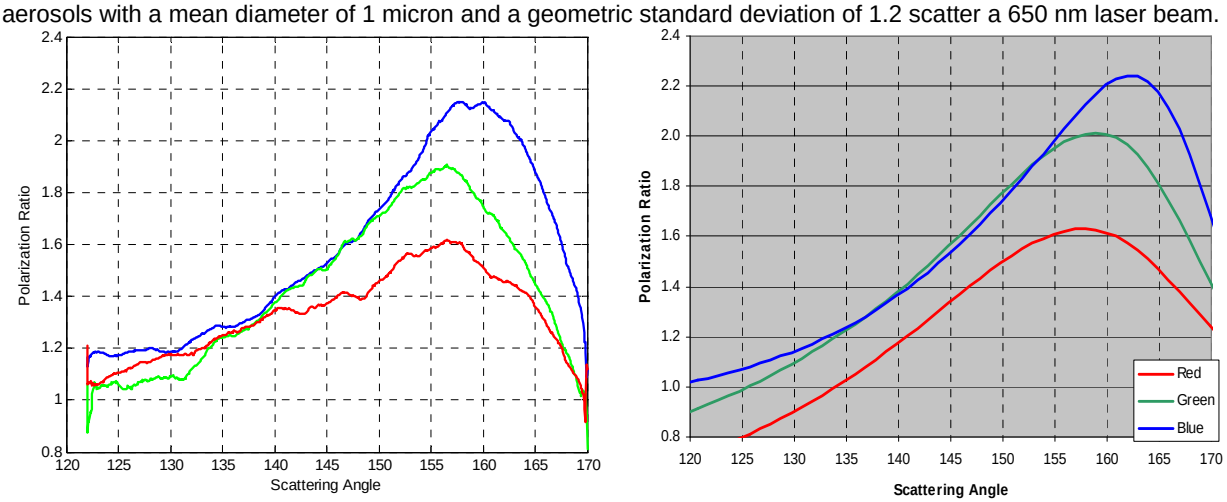

Figure 15. Measurements (left side) and calculations (right side) represent the results from a fog oil experiment with a mean diameter of ~230 nm and geometric standard deviation of 1.66 in the Penn State Aerosol Chamber in July 2009 (Brown et al. 2010; Brown 2010).

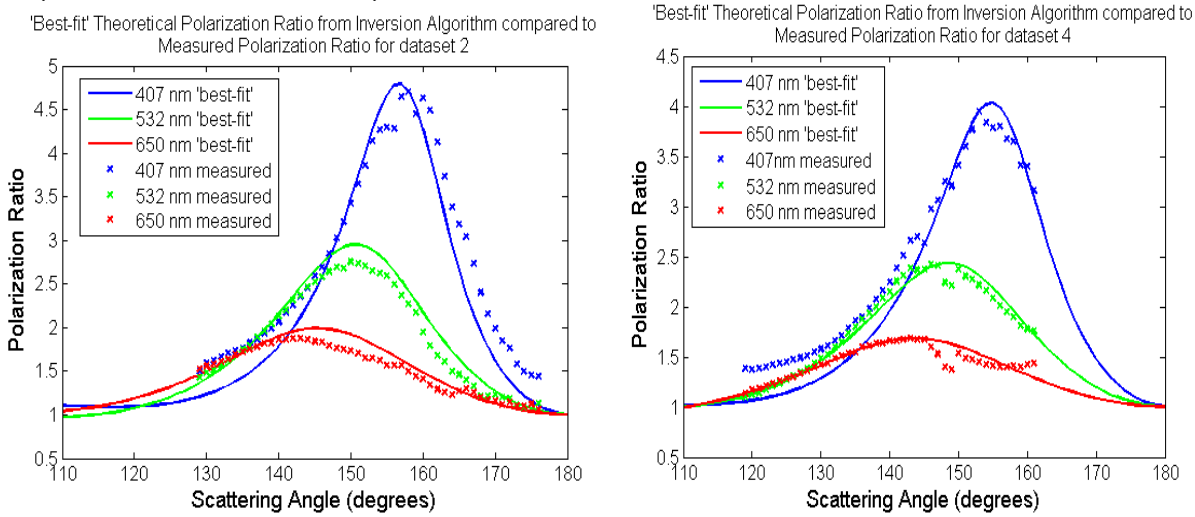

Figure 16. Measurements and calculations of polarization ratios for two chamber tests at the EPA Aerosol Chamber using three wavelengths (Brown et al. 2010; Brown 2010).

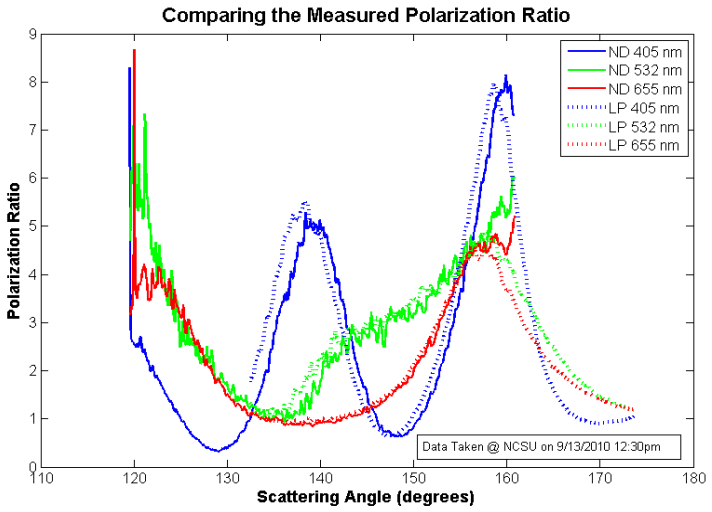

Figure 17. Polarization Ratio of the scattering phase function measured for 1 μm polystyrene spheres using two cameras.

6. SUMMARY

Rayleigh and Raman lidar signals scattered from molecules and aerosols provide backscatter and extinction profiles that describe the atmospheric optical properties controlling radiative transfer through the atmosphere. Additionally, a laser beam can be used in bistatic and multistatic techniques to obtain measurements of the polarization ratio of the scattering phase function. Analyses of multistatic measurements determine profiles of the aerosol number density, size, size distribution, and type. These parameters can be determined for spherical particles in the size range between about 20 nm and 20 μm. Additional information on aerosol type and shape can be determined from the approximate refractive index of the scattering aerosols and by measuring the depolarization of the scattered radiation. DIAL lidar, hyper-spectral sensors, multi-wavelength lidar, the recent use of supercontinuum lasers, and efforts with resonance Raman scatter techniques are expanding the remote sensing capabilities, particularly for identifying and measuring trace concentrations of species needed to describe the optical absorption affecting the radiation balance. The optimum system being currently considered is a 4-λ instrument using the 1064, 532, and 355 nm wavelengths of an Nd:YAG laser and a 4 μm MWIR laser, see Fig. 18.

The initial development of the bistatic lidar technique that images an angular range of the scattering from a laser beam and uses the polarization ratio of the scattering phase function to analyze the results was accomplished by Stevens (Stevens and Philbrick, 1996a, 1996b, Stevens 1996). A major advance in our use of the scattering information resulted from the work of Novitsky (Novitsky 2002, Novitsky and Philbrick 2005), with the multistatic lidar system. The technique has been extended to the case of aerosol multiple scattering and resulted in useful experimental and theoretical advances (Park 2008, Park and Philbrick 2008). The next advances are underway by making use of multi-wavelength scattering using several laser wavelengths simultaneously; even the case of using a supercontinuum laser is studied (Wyant et al. 2009, Brown 2010). The investigations of aerosols are being combined with measurements of other meteorological parameters from Raman lidar and Differential Absorption Spectroscopy (DAS) to examine the optical properties through the optical spectrum (Philbrick et al, 2009a, 2009b).

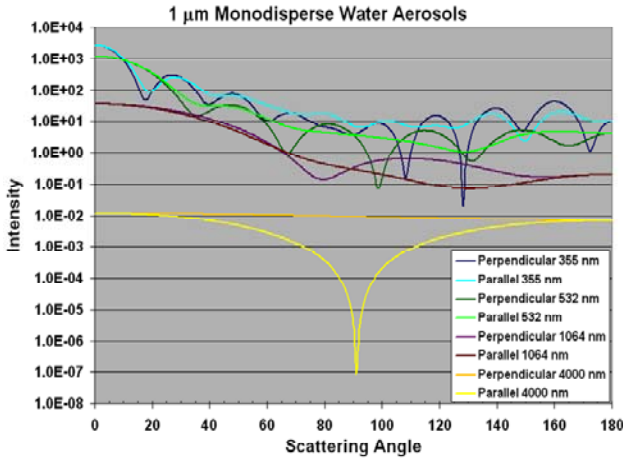

Figure 18. The scattering phase functions for 1 mm water aerosols are plotted for a 4-λ bistatic lidar.

7. REFERENCES

Born, Max and Emil Wolf, 2002: Principles of Optics, Cambridge University Press, New York.

Brown, Andrea M., Michelle G. Snyder, Lydia Brouwer, and C. Russell Philbrick, 2010: "Atmospheric aerosol characterization using multi-wavelength, multi-static light scattering," Laser Radar Technology and Applications XIV, Proc. of SPIE Vol. 7684, doi: 10.1117/12.850080.

Brown, Andrea M., 2010: PhD Dissertation, Department of Electrical Engineering, Penn State University.

Li, Guankun, and C. Russell Philbrick, 2002: "Lidar Measurements of Airborne Particulate Matter," in Remote Sensing of the Atmosphere, Environment, and Space, SPIE , 4893-15.

Mulik, Karoline R., 2000: Evolution of ozone and particulate matter during pollution events using Raman lidar. Penn State University MS Thesis, Electrical Engineering Department, 68 pgs.

Novitsky, E. J., and C.R. Philbrick, 2005: "Multistatic Lidar Profiling of Urban Atmospheric Aerosols," J. Geophy. Res. - Atmospheres, 110, DO7S11.

Novitsky, Edward J., 2002 PhD Dissertation, Department of Electrical Engineering, Penn State University.

O'Brien, M.D. T. D. Stevens and C. R. Philbrick, 1996: "Optical Extinction from Raman Lidar Measurements," Optical Instruments for Weather Forecasting, SPIE Proc. 2832, 45-52.

Park, Jin H., and C. Russell Philbrick, 2006: "Multiple Scattering Measurements Using Multistatic Lidar," Proc. International Aerosol Conference.

Park, Jin H., 2008: PhD Dissertation, Department of Electrical Engineering, Penn State University.

Philbrick, C.R., 2002a: "Raman Lidar Descriptions of Lower Atmosphere Processes," Lidar Remote Sensing in Atmospheric and Earth Sciences, Proc. 21st ILRC, Valcartier, Quebec Canada, 535-545.

Philbrick, C. Russell, 2002b: "Overview of Raman Lidar Techniques for Air Pollution Measurements," Lidar Remote Sensing for Industry and Environment Monitoring II, SPIE , 136-150.

Philbrick, C.R., 2005: "Raman Lidar Characterization of the Meteorological, Electromagnetic and Electro-optical Environment," Proc. SPIE Vol. 5887, Lidar Remote Sensing for Envir. Monitoring VI, p. 85-99.

Philbrick, C. Russell, David M. Brown, Adam H. Willitsford, Perry S. Edwards, Andrea M. Wyant, Zhiwen Z. Liu, C. Todd Chadwick, and Hans Hallen, 2009a: "Remote Sensing of Chemical Species in the Atmosphere" *Proc. of Fourth Symposium on Lidar Atmospheric Applications*, as part of the 89th AMS Annual Meeting http://ams.confex.com/ams/pdfpapers/150051.pdf

Philbrick, C. Russell, Hans Hallen, 2009b: "Measurements of Contributors to Atmospheric Climate Change," Proc. 19th Symposium on European Rocket and Related Research, ESA Special Publication SP-671.

Reagan, J.A., D.M. Byrne and B.M. Herman, 1982a: "Bistatic LIDAR: A Tool for Characterizing Atmospheric Particulates: Part I – The Remote Sensing Problem," IEEE Geo. Remote Sensing 20, 229.

Reagan, J.A., D.M. Byrne and B.M. Herman, 1982b: "Bistatic LIDAR: A Tool for Characterizing Atmospheric Particulates: Part II – The Inverse Problem," IEEE Geosciences and Remote Sensing 20, 236.

Stevens, T.D., and C. R. Philbrick, 1996a: "Particle Size Distributions and Extinction Determined by a Unique Bistatic Lidar Technique," Proceeding of IGARSS96 Conference on Remote Sensing for a Sustainable Future (International Geophysics and Remote Sensing Symposium) II, 1253-1256.

Stevens, T.D., and C. R. Philbrick, 1996b: "A Bistatic Lidar Receiver to Observe Lower Tropospheric Aerosol Properties," Proceedings of the 18th Annual Conference on Atmospheric Transmission Models, 6-8 June 1995, PL-TR-96-2080, Special Report 278, Phillips Laboratory, Hanscom AFB MA 01731, 242.

Stevens, Timothy D., 1996: PhD Dissertation, Department of Electrical Engineering, Penn State University.

Verghese, Sachin J., Adam H. Willitsford and C. Russell Philbrick, 2005: "Raman Lidar Measurements of Aerosol Distribution and Cloud Properties," Lidar Remote Sensing for Environmental Monitoring VI, edited by Upendra N. Singh, Proc. of SPIE Vol. 5887 H-1.

Verghese, Sachin, 2008: PhD Dissertation, Department of Electrical Engineering, Penn State University.

Wyant, Andrea M., David M. Brown, Perry S. Edwards, and C. Russell Philbrick, 2009: "Multi-wavelength, multi-angular lidar for aerosol characterization" Laser Radar Technology and Applications XIV, Proc. of SPIE Vol. 7323.